Molecular drug design, synthesis and structure elucidation of a new specific target peptide based metallo drug for cancer chemotherapy as topoisomerase I inhibitor

ARTICLE *in* DALTON TRANSACTIONS · MARCH 2012

Impact Factor: 4.2 · DOI: 10.1039/c2dt12044e · Source: PubMed

Dalton Transactions

Cite this: *Dalton Trans.*, 2012, **41**, 4955

www.rsc.org/dalton

PAPER

Molecular drug design, synthesis and structure elucidation of a new specific target peptide based metallo drug for cancer chemotherapy as topoisomerase I inhibitor†

Sartaj Tabassum,*[a] Waddhaah M. Al-Asbahy,[a] Mohd. Afzal,[a] Farukh Arjmand[a] and Vivek Bagchi[b]

Received 27th October 2011, Accepted 13th February 2012
DOI: 10.1039/c2dt12044e

To evaluate the biological preference of metallopeptide drugs in cancer cells, a new dinuclear copper(II) complex $[Cu_2(glygly)_2(ppz)(H_2O)_4]\cdot 2H_2O$ (**1**) (glygly = glycyl glycine anion and ppz = piperazine), was designed and synthesized as topoisomerase I inhibitor. The structural elucidation of the complex was done by elemental analysis, spectroscopic methods and single crystal X-ray diffraction. The *in vitro* DNA binding studies of complex **1** with CT DNA were carried out by employing different optical methods *viz.* UV-vis, fluorescence and circular dichroism. The molecular docking technique was also utilized to ascertain the mechanism and mode of action towards the molecular target DNA and enzymes. Complex **1** cleaves pBR322 DNA *via* an oxidative mechanism and strongly binds to the DNA minor groove. Furthermore, complex **1** exhibits significant inhibitory effects on the catalytic activity of topoisomerase I at a very low concentration, ~12.5 μM, in addition to its excellent SOD mimics (IC_{50} ~ 0.086 μM).

Introduction

Cancer – a growing menace (total global cancer 2008: 12 662 554; 2030: +69%) – is a complex disease of which many people are afraid, and cancer – the big C – will often top the list as the major cause of morbidity and mortality of mankind. In a recent report in *Nature*, cancer surpassed all other causes of mortality, outweighing all other health concerns *viz.* cardiovascular diseases, cerebrovascular diseases, HIV/AIDS, lower respiratory infection including pneumonia, malaria, and cirrhosis, as well as road accidents.[1] Therefore, an important challenge for chemists today is in the area of medicinal chemistry, to develop new drugs for treating chronic diseases which show promise (i) to increase the survival rates of patients, (ii) to reduce the systemic dose-limiting toxicity arising from off-target binding at the molecular level, (iii) possess a mechanism for resistance development, (iv) exhibit superior chemical and pharmacological properties (good solubility, cellular uptake, kinetically stable and robust molecules, specific binding domain and good metabolic clearance).[2]

Metal complexes have been extensively explored for anticancer activities after the protocol success of cisplatin for treating most aggressive solid tumors.[3] Many of these chemotherapeutic agents act by inhibition of the synthesis of deoxyribonucleic acid DNA, a natural target due to its predominant role in cellular replication. However, the chemical entities which exhibit different mechanisms of action are gaining more importance. DNA inhibition can be achieved by direct DNA binding in either a covalent interaction due to an outer-sphere or inner-sphere binding and consecutive strand breakage, external electrostatic binding and groove-face binding or a noncovalent interaction by intercalation.[4] Studies on the noncovalent interactions of small molecules with the minor groove of DNA are promising as potential new therapeutic agents.[5]

Topoisomerase I is a nuclear enzyme that catalyzes the topological changes of DNA during replication, transcription, recombination, repair, chromatin assembly and chromosome segregation by triggering single-stranded breaks in DNA.[6] The literature reveals that minor groove analogs such as camptothecin (currently used as an anticancer drug), Hoechst 33258, bleomycin and netropsin (G–C recognition elements) emerged as important antineoplastic and antiproliferative agents.[7] The bithiazole moiety of bleomycin which is a naturally occurring metallopeptide binds to DNA by alkylation or cleavage of DNA or indirectly *via* inhibition of topoisomerase activities.[8] Herein, we aim to design anticancer drug entity **1** – a dinuclear copper(II) dipeptide piperazine bridged complex capable of recognizing a specific sequence in DNA minor groove to inhibit the expression of topoisomerase I and thereby, control the replication of tumor cells. Heterocyclic compounds containing the piperazine moiety are gaining immense interest owing to their biological and pharmacological properties *viz.* excellent Gram-negative potency, good therapeutic plasma levels in animals and man, 5-HT_{1A}R

[a]*Department of Chemistry, Aligarh Muslim University, Aligarh 202201, UP, India. E-mail: tsartaj62@yahoo.com; Tel: +91 9358255791*
[b]*Department of Chemistry, University of Missouri, Rolla, MO 65409, USA*

†Electronic supplementary information (ESI) available: packing diagrams, agarose gel electrophoresis pattern for minor groove binding, molecular docked model of complex **1** in DNA sequence between C112, A113 and T10, TGP11 of Topo-I, Key-lock interaction with SOD enzyme. CCDC reference number 794697. For ESI and crystallographic data in CIF or other electronic format see DOI: 10.1039/c2dt12044e

agonists and, most notably, their antitumor activity.[9,10] Complex **1** exhibits novelty, fulfilling all the pre-requirements for efficient chemotherapeutic drug design which include (i) a well-defined complex shape and metal binding domain, (ii) cleaving DNA oxidatively in a fashion reminiscent of the bleomycin group which is a clinically employed antitumor agent[11] and potent Topo-I inhibitor activity, (iii) increased bio-activity due to multi-faceted binding modes (groove interaction; hydrogen bonding interaction with specific bases; hydrophobic interaction and electrostatic interaction between negatively charged groove surface and amino functionality of dipeptide), (iv) may act as immuno-modulators by changing numbers and immune cells and thus affect (activate or suppress) cytotoxic immune response,[12] (v) its dinuclear metal active centers received much attention towards catalyzing the dismutation of superoxide anions to oxygen and hydrogen peroxide under physiological conditions. A computer-aided molecular docking study was carried out in this work to validate the specific groove binding mode, in addition to Topo-I and SOD activity at the molecular level.

Results and discussion

Synthesis and characterization

In order to enhance the specificity of the molecular recognition towards DNA helices and inhibition of the catalytic activity of many enzymes, a new drug candidate, complex **1** was synthesized and characterized. The synthesis of the new dinuclear copper(II) complex **1** was achieved by mixing stoichiometric amounts of Cu(II) nitrate trihydrate with glycyl glycine followed by reaction with piperazine hexahydrate (Scheme 1). The resulting complex **1** is stable towards air and moisture and readily soluble in H_2O. The complex was characterized by elemental analysis, IR, UV-vis and EPR spectral studies. The molar conductance value of the complex in H_2O (1×10^{-3} M) at 25 °C suggest its non-electrolyte nature (20 Ω^{-1} cm^2 mol^{-1}). The formulation of the complex **1** was further confirmed by determination of the X-ray crystal structure.

Description of crystal

The single crystal X-ray analysis reveals that the complex **1** crystallizes as a monoclinic crystal system with space group *P*21/*c*. An ORTEP view of the complex is illustrated in Fig. 1, while selected bond lengths and bond angles are listed in ESI Table S1.† The packing diagram in the unit cell is shown in Fig. S1.† The complex **1** contains two six coordinated Cu(II) centers bridged by a piperazine ligand, which adopted a chair-shape conformation at the equatorial site. Both Cu(II) centers are in a N_3O_3 coordination environment arranged in distorted octahedral geometries, as evidenced by all of the angles around them, which deviate from 180° and 90° (Table S1†). The coordination sites around each Cu(II) center are achieved by the terminal amino nitrogen (Cu(1)–N(2), 2.063 Å), the deprotonated peptide nitrogen (Cu(1)–N(2), 1.897 Å) and one of the carboxylate oxygens (Cu(1)–O(1), 2.017 Å) of the dipeptide and the fourth is ligated by the piperazine nitrogen (Cu(1)–N(3), 1.993 Å). Besides these coordinations, the axial position is occupied by two oxygen atoms, O4 and O5 (Cu(1)–O(4), 2.381 Å, Cu(1)–O(5), 2.381 Å) provided by aqua ligands. The Cu–N_{imine} distances (involving sp^2 N) are slightly shorter than the Cu–N_{amine} distances (involving sp^3 N), indicating that deprotonated nitrogen is more strongly coordinated to the metal center than the terminal amino group.[13,14] On the other hand, the Cu–$O_{carboxylate}$ bond lengths exhibit smaller values than the Cu–O_{water}. The intramolecular Cu···Cu distance is near 6.803 Å, which is short as compared to 6.908 and 6.881 Å in previously reported chair-piperazine-bridged Cu_2 complexes.[15] The small bite angles of N(1)–Cu(1)–N(2) and N(1)–Cu(1)–O(1) of 82.44° and 82.38°, respectively, are primarily responsible for distortion from the regular octahedral geometry. Whereas, the angles between N(1)–Cu(1)–N(3), N(3)–Cu(1)–O(1), N(3)–Cu(1)–N(2), O(1)–Cu(1)–N(2) and N(1)–Cu(1)–O(4) are 173.20°, 98.77°, 95.56°, 163.48° and 92.83°, respectively. The stability of the complex is reinforced by the intra-molecular interligand interaction (ppz) N3–H3···O2 (glygly) (2.079 Å; Fig. S1†).

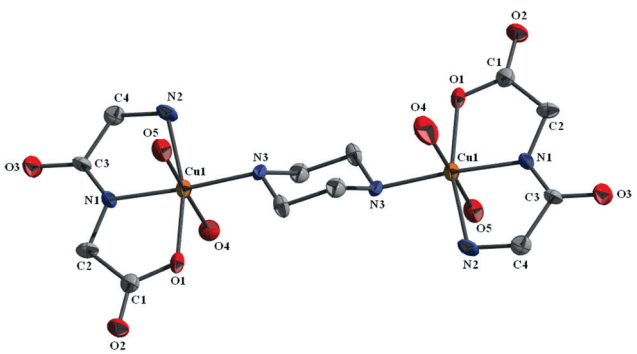

Fig. 1 The molecular structure of complex **1**, $[Cu(glygly)_2(ppz)(H_2O)_4]\cdot 2H_2O$; thermal ellipsoids are drawn at 50% probability level and solvent molecules are omitted for clarity.

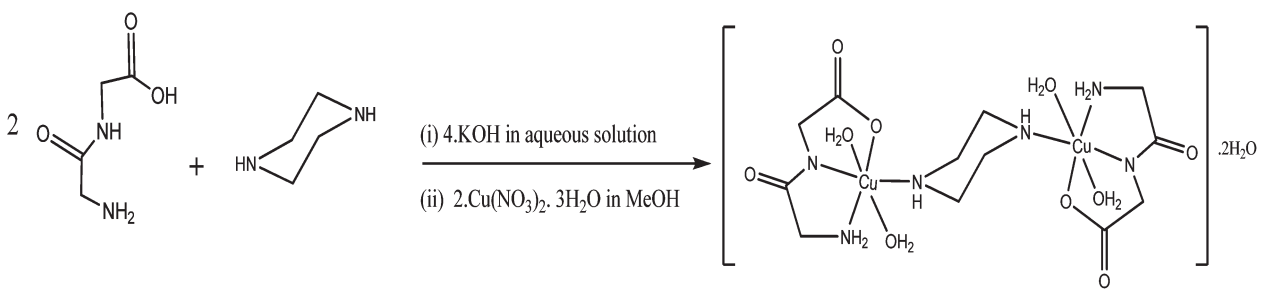

Scheme 1 The synthetic route for complex **1**.

Thus, the molecular recognition pattern between the Cu(ppz) chelate and the glygly ligand is featured by the cooperative effect of the Cu(1)–N3(ppz) coordination bond and referred as an inter-ligand H-bond. Moreover, it seems clear that such an intra-molecular H-bond noticeably influences the molecular topology.[16]

Furthermore, it is believed that the mode of coordination has a major influence on the conformational changes of a peptide molecule that influences its reactivity towards the receptor sites. So, complex formation plays significant role in the biological activity of peptides where metal ions can be regarded as catalysts for many reactions and have been used for DNA selective recognition and/or cleavage.

Infrared spectra

The assignment of the IR bands of complex **1** was carried out in comparison to the IR spectra of the free dipeptide. The formation of the complex was evidenced by the appearance of characteristic absorption bands at 3100–2950, 1625–1600, 1585–1550 and 1393–1348 cm^{-1}, which were attributed to $\nu_{as}(NH_3^+)$, $\delta(NH_3^+)$, $\nu_{as}(CO_2)$ and $\nu_s(CO_2)$, respectively. The disappearance of the $\nu_{as}(NH_3^+)$, and $\delta(NH_3^+)$ bands (associated with the zwitterions structure) in complex **1** was coupled with the appearance of a broad band in the range 3398–3267 cm^{-1} assigned to the stretching vibrations of coordinated water molecules and terminal amino groups. The $\nu(CO)_{peptide}$ [amide I] band observed at ~1665 cm^{-1} in the free dipeptide was shifted to lower frequency at ~1602 cm^{-1} in complex **1** after complexation, confirming the coordination of the metal ion through an O atom of a deprotonated carboxylate group.[17,18] The bands around 1575 and 1254 cm^{-1} observed in the free dipeptides are attributed to amide II and III bands [due to δ(NH) + ν(C–N) in the compound containing neutral secondary peptide groups] were replaced by a new absorption band at 1376 cm^{-1} in complex **1**. This is characteristic for a deprotonated secondary peptide complex, since on removal of peptide proton the band becomes a pure C–N stretch.[19] The formation of complex **1** was also revealed by the presence of intense bands around ~415 and ~537 cm^{-1} corresponding to Cu–N and Cu–O, respectively.

Electronic spectra

The electronic absorption spectrum of complex **1** in freshly prepared aqueous solution was obtained in the region 200–1100 nm at room temperature. The electronic spectra of free dipeptides displayed intense absorption bands at 220 nm due to an $n \rightarrow \pi^*$ transition which was shifted to 232 nm upon coordination with Cu(II) metal ion, and has been assigned to a $N^- \rightarrow$ Cu(II) ligand-to-metal charge transfer (LMCT) transition. A band at 278 nm was tentatively assigned to a $COO^- \rightarrow$ Cu(II) charge-transfer transition.[17,20] The low energy d–d band at 644 nm was assigned to $^2B_{1g} \rightarrow {}^2B_{2g}$ transitions suggesting an octahedral geometry around the Cu(II) metal ion,[21] as deduced by EPR and validated by the X-ray crystal structure.

EPR studies

The solid state X-band EPR spectrum of complex **1** was acquired at a frequency of 9.1 GHz under the magnetic field strength 3000 ± 1000 Gauss using tetracyanoethylene (TCNE) as field marker at LNT. The complex shows an anisotropic spectrum with $g_{\|} = 2.19$ and $g_{\perp} = 2.06$ and $g_{av} = 2.08$ computed from the expression $g_{av}^2 = (g_{\|}^2 + 2g_{\perp}^2)/3$. These values are consistent with an octahedral geometry of copper with d^9 (Cu^{II}) configuration *i.e.* $(eg)^4$ $(a1g)^2$ $(b2g)^2$ $(b1g)^1$, occupied by an unpaired electron. The trend $g_{\|} > g_{\perp} > g_e$ (2.0023) reveals that the unpaired electron is localized in the orbital.[22] For a Cu(II) complex, $g_{\|}$ is a parameter sensitive enough to indicate covalence. For a covalent complex, $g_{\|} < 2.3$ and for an ionic environment, $g_{\|} = 2.3$ or more. In the present complex $g_{\|} < 2.3$ indicates an appreciable metal–ligand covalent character.[23] The exchange interaction parameter $G < 4$ (1.89), indicates considerable exchange interaction between the Cu(II) centers in the solid phase.[24]

DNA binding studies

Electronic absorption titration

Electronic absorption spectroscopy is an effective method to examine the binding modes of complexes with DNA followed by the changes in the absorbance and shift in the wavelength. The absorption spectra of complex **1** in the absence and presence of CT DNA are shown in Fig. S2.† Binding of the complexes to DNA is expected to perturb the ligand centered transitions of complexes. Upon the addition of increasing amounts ($0.067–0.33 \times 10^{-4}$ M) of CT DNA to complex **1** of fixed concentration (0.067×10^{-4} M), there was an increase in the absorption intensity of complex **1** indicative of hyperchromism with no band shift. Hyperchromism with no shift in absorbance is consistent with groove binding, therefore in this complex it can be attributed to external contact (surface binding) with the duplex through hydrogen-bonding interactions between coordinated –NH and $–NH_2$ with functional groups positioned on the edge of DNA bases which are accessible both in the major and minor grooves or due to strong binding of the complex to CT DNA possibly *via* electrostatic interactions indicating DNA stabilization.[25,26] These results suggest the possibility of groove binding for the complex **1** to DNA and clearly rule out the intercalative binding of the complex to DNA, as the intercalation mode of binding leads to "hypochromism" in the spectral bands.[27] Complex **1** possesses coordinated –NH– piperazine and amino functionalities of the dipeptide (glygly), which are quite likely to be engaged in hydrogen bonding with H-bond acceptor groups (the purine N(3) and pyrimidine O(2) at the floor of the groove walls). To assess the binding ability of the complex **1** with CT DNA, the intrinsic binding constant (K_b) value was calculated and found to be 2.14×10^5 M^{-1}. The K_b values suggest that complex **1** has a strong binding affinity for CT DNA, which is further validated by the molecular docking technique.

Ethidium bromide displacement assay

No luminescence was observed for the complex **1** at room temperature in aqueous solution, in any organic solvent, or in the presence of CT DNA. So, the binding of complex **1** with DNA cannot be directly predicted through the emission spectra. Therefore, interaction of the complex **1** with DNA was carried out by a

competitive binding experiment using ethidium bromide (EB) as a probe. EB does not show any appreciable emission in the buffer solution due to fluorescence quenching of the free EB by solvent molecules, while in the presence of CT DNA, the fluorescence intensity of EB was highly enhanced due to its strong intercalation between the adjacent DNA base pairs.[28] The addition of a second DNA-binding molecule can quench the emission intensity of a DNA–EB adduct by either replacing the EB and/or by accepting the excited-state electron of the EB through a photoelectron transfer mechanism.[29] The addition of complex **1** to DNA pretreated with EB (Fig. S3†) caused a significant reduction in emission intensities, which indicated that the complex **1** could bind to DNA through the groove binding mode releasing some EB molecules from the EB–DNA system.[30] The extent of reduction of the emission intensity gives a measure of the binding propensity of the complex **1** to CT DNA. According to the classical Stern–Volmer equation

$$I_0/I = 1 + K_{SV}r$$

where I_0 and I represent the fluorescence intensities in the absence and presence of the complex **1**, respectively; r is the concentration ratio of the complex to DNA, and K_{SV} is used to evaluate the quenching efficiency and is obtained as the slope of I_0/I *vs.* r. The K_{SV} value for the complex **1** was found to be 2.15, indicating the strong affinity of the complex **1** to CT DNA, consistent with the studies of absorption titrations.

Circular dichroism spectral study

CD spectroscopy is a useful technique in diagnosing changes in DNA morphology during drug–DNA interactions. The CD spectrum of CT DNA exhibits a positive band at 275 nm (UV: λ_{max}, 260 nm) due to base stacking and a negative band at 245 nm due to the right-handed helicity of the B-DNA form which are quite sensitive to the mode of DNA interactions with small molecules. Simple groove binding and electrostatic interaction of the complexes with DNA shows less or no perturbation of the base stacking and helicity bands, while an intercalator enhances the intensities of both bands.[31,32] The interaction of the complex **1** with DNA induces a change in the CD spectrum of B-DNA (Fig. 2). The intensities of both the negative and positive bands decrease significantly (shifting to zero levels). This suggests that the DNA binding of the complex induces certain conformational changes, such as the conversion from a more B-like to a more C-like structure within the DNA molecule.[33] From the results of UV absorption, fluorescence and CD spectroscopic studies, we conclude that the complex **1** avidly binds to CT DNA.

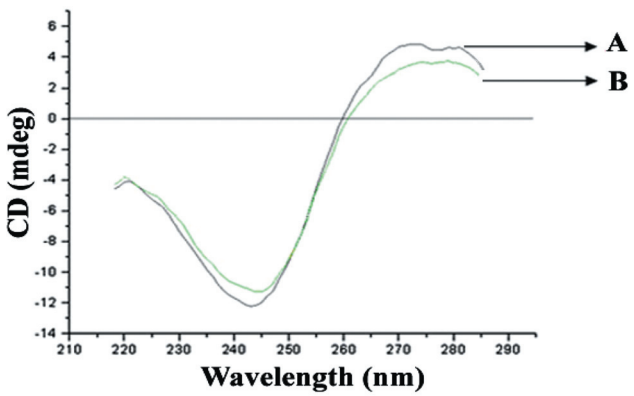

Fig. 2 CD spectra of (A) CT DNA alone (B) CT DNA in the presence of complex **1** in 5 mM Tris-HCl/50 mM NaCl buffer at 25 °C. [Complex] 1.0×10^{-4} M, [DNA] 1.0×10^{-4} M.

DNA cleavage studies

Without added reductant (concentration dependent)

In order to assess the chemical nuclease activity of the copper(II) complex for DNA strand scission, pBR322 DNA was incubated with the copper(II) complex under the reaction conditions. The cleavage reaction can be monitored by gel electrophoresis. When circular plasmid DNA is conducted by electrophoresis, the fastest migration will be observed for the supercoiled form (Form I). If one strand is cleaved, the supercoils will relax to produce a slower-moving nicked circular form (Form II). If both strands are cleaved, a linear form (Form III) that migrates between Form I and Form II will be generated.[34]

The nuclease activity of the complex has been studied by agarose gel electrophoresis using supercoiled pBR322 plasmid DNA in a medium of 5 mM Tris-HCl/50 mM NaCl buffer solution (pH 7.2) in the absence of external agents. The cleavage reactions have been studied using different complex concentrations incubated at 310 K for 45 min as depicted in Fig. 3. With increasing the concentration of the complex **1** (lanes 2–4), the amount of Form I of pBR322 DNA diminishes gradually, whereas Form II increases. At the same time, when the concentration of complex **1** reached 25 μM, the linear Form III was manifested in the gel (lane 5), and the percentage of linear DNA increased with the increase of the concentration of complex **1**. So, it is clear that cleavage of pBR322 DNA is highly dependent on the metal ions concentration.

DNA cleavage in presence of activators

To ascertain whether any adventitious agents present in the reaction mixture could account for the increased DNA degradation by complex **1**, the DNA cleavage activity was studied in the presence of activators. The nuclease efficiency of the copper(II) complexes is known to depend on the activators used for initiating the DNA cleavage. Thus, further activity of complex **1** has been studied with different activators *viz.* H_2O_2 as an oxidizing agent, ascorbate (Asc), 3-mercaptopropionic acid (MPA) and glutathione (GSH) as reducing agents. As shown in Fig. 4 (lanes 2–5), the cleavage activity of complex **1** was significantly

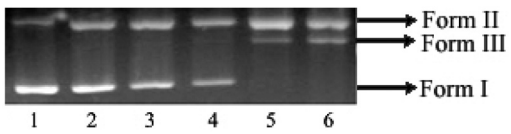

Fig. 3 Agarose gel electrophoresis patterns for the cleavage of pBR322 supercoiled DNA (300 ng) by complex **1** at 310 K after 45 min of incubation; lane 1, DNA control; lane 2, 10 μM of **1** + DNA; lane 3: 15 μM of **1** + DNA; lane 4: 20 μM of **1** + DNA; lane 5: 25 μM of **1** + DNA; lane 6: 30 μM of **1** + DNA.

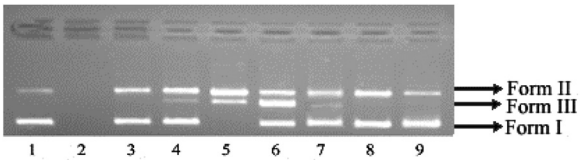

Fig. 4 Agarose gel electrophoresis patterns for the cleavage of pBR322 supercoiled DNA (300 ng) by complex **1** in presence of different activating agents at 310 K after incubation for 45 min. lane 1: DNA control; lane 2: 25 μM of **1** + H_2O_2 (0.4 M) + DNA; lane 3: 25 μM of **1** + MPA (0.4 M) + DNA; lane 4: 25 μM of **1** + GSH (0.4 M) + DNA; lane 5: 25 μM of **1** + Asc (0.4 M) + DNA; lane 6: 25 μM of **1** + DMSO (0.4 M) + DNA; lane 7: 25 μM of **1** + ethyl alcohol (0.4 M) + DNA; lane 8: 25 μM of **1** + sodium azide (0.4 M) + DNA lane 9: 25 μM of **1** + SOD (15 units) + DNA.

enhanced in the presence of these activators and follows the order H_2O_2 > MPA > Asc ≈ GSH. Thus, complex **1** exhibited a significant DNA cleavage activity in the presence of H_2O_2.

The mechanistic pathway proposed for the interaction of complex **1** with DNA in the presence of H_2O_2 is illustrated as:

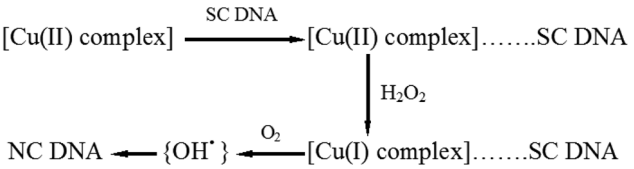

Reactive oxygen species responsible for DNA cleavage

Copper complexes can cleave DNA both by hydrolytic and/or oxidative mechanisms. For the oxidative process, the complexes have been shown to react with molecular oxygen or hydrogen peroxide to produce a variety of active oxidative intermediates (reactive oxygen species or non-diffusible copper-oxene species).[35] In order to gain information about the reactive oxygen species (ROS) which was responsible for the DNA cleavage catalyzed by the complex **1**, reactions were carried out in the presence of typical scavengers such as hydroxyl radical scavengers (DMSO, EtOH), a singlet oxygen quencher (NaN_3) and a superoxide scavenger (SOD) under our experimental conditions. As shown in Fig. 4, the DNA breakdown mediated by complex **1** was diminished in presence of DMSO (lane 6) and EtOH (lane 7), which indicates that the hydroxyl radical participates in the oxidative DNA cleavage. Sodium azide had no significant effect on the DNA cleavage (lane 8). This fact rules out the participation of $^1O_2$ or singlet oxygen-like entities.[36] On the other hand, DNA cleavage was inhibited slightly in presence of SOD (lane 9), which demonstrates the involvement of the superoxide radical anion ($O_2^{\cdot -}$) in DNA strand scission suggestive of an oxidative cleavage mechanism.[37] From these results, we can conclude that a Cu(I) species, superoxide O_2 and hydroxyl radical $OH^{\cdot}$ are the active species involved in the DNA strand scission.

DNA cleavage in presence of recognition elements (groove binding)

To determine the groove binding preference of the complex **1** with pBR322 DNA, the supercoiled pBR322 DNA was treated with DNA groove binders such as DAPI (minor groove binding agent) and methyl green (major groove binding agent) prior to the addition of complex **1**. As shown in Fig. S4,† DNA cleavage is inhibited in the presence of DAPI (lane 2). However, no apparent inhibition of DNA damage was observed in the presence of methyl green (lane 3), suggesting that the complex has interaction with DNA through the small groove, which is further validated by molecular docking studies.

Topoisomerase I inhibition

A plasmid DNA cleavage assay was used to investigate the effect of complex **1** on the activity of human Topo-I by agarose gel electrophoresis. This assay provides a direct means of determining whether the drug affects the unwinding of a supercoiled (SC) duplex DNA to nicked open circular (NOC) and relaxed (R) DNA. When the catalytic activity of topoisomerase I was assayed, complex **1** inhibited this process in a concentration-dependent manner.[38] As shown in Fig. 5, supercoiled DNA was fully relaxed by the enzyme in the absence of complex **1** (lane 2, Topo-I). However, upon increasing the concentration of complex **1** (5–12.5 μM), the levels of relaxed form were inhibited (lanes 3–6). At 12.5 μM the DNA relaxation effect caused by Topo-I was completely inhibited by complex **1**. These observations suggest that complex **1** inhibits topoisomerase I catalytic activity due to the relatively strong DNA binding affinity of complex **1**, which prevents the enzyme from efficiently binding to the DNA. Thus, the metal-based drug entity can exert its antitumor activity *via* topoisomerase I inhibition as it was found that most of the cancer cells (kidney, colon, prostate, ovary and esophagus) showed significantly increased levels of topoisomerase, which is required for rapid and unchecked proliferation of cancer cells.[39]

Superoxide dismutase activity

Superoxide dismutase (SOD) is one of the most crucial enzymes in the defense system of organisms for its ability to protect cells from the damage of the toxic superoxide by catalyzing the dismutation of superoxide radicals effectively.[40] Therefore, it was interesting to investigate the SOD-like activity of this new dipeptide based binuclear Cu(II)-complex by using the xanthine–xanthine oxidase–nitroblue tetrazolium (NBT) assay. A plot of NBT percent inhibition with an increase in concentration of complex **1** is presented in Fig. 6. ESI Table S2† shows the

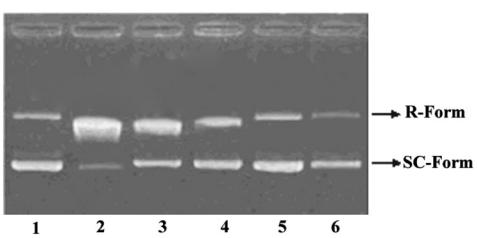

Fig. 5 Agarose gel electrophoresis patterns showing the effect of different concentrations of complex **1** on the activity of DNA topoisomerase I (Topo-I); lane 1, DNA control; lane 2, Topo-I + DNA; lane 3, 5 μM of **1** + DNA + Topo-I; lane 4: 7.5 μM of **1** + DNA + Topo-I; lane 5: 10 μM of **1** + DNA + Topo-I; lane 6: 12.5 μM of **1** + DNA + Topo-I.

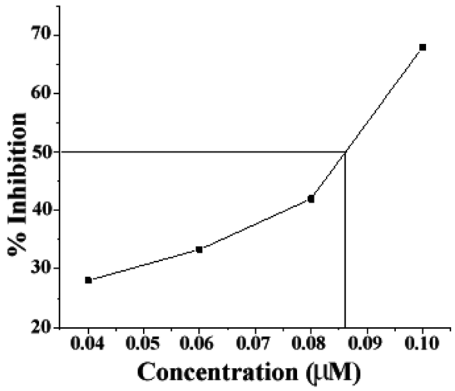

Fig. 6 A plot of percentage of NBT inhibition reduction with an increase in the concentration of complex **1**.

concentration of complex **1** necessary to produce 50% inhibition (IC_{50}) of the reaction together with the values found for the previously investigated dipeptide complexes and the one obtained with native SOD.[41] The IC_{50} value of complex **1** is 0.086 μM, which is considered to be an excellent SOD mimic among the most active dipeptide complexes but it is somewhat less active than the IC_{50} value obtained for native enzyme (IC_{50} = 0.04 μM). In the enzyme, the flexible dipeptides together with piperazine ligand can accommodate and stabilize the space structure of the protein and provide needed protons to the peroxide anion during the catalytic cycle. Since the proton exchange between substrates and buffer is a rapid process in the small model systems, the buffer can directly transfer protons to peroxide anion in the mechanism.[42]

$$Cu(II) + O_2^{\cdot -} \rightleftharpoons Cu(I) + O_2$$

$$Cu(I) + O_2^{\cdot -} + 2H^+ \rightleftharpoons Cu(II) + H_2O_2$$

Furthermore, the high superoxide dismutase activity of complex **1** may be possibly due to cooperation of two Cu(II) centers in close proximity, acting in concord in free radical binding and electron transfer.

Molecular docking

Molecular docking with DNA

Molecular docking techniques are an attractive scaffold to understand the drug–DNA interactions in rational drug design, as well as in the mechanistic study by placing a small molecule into the binding site of the target specific region of the DNA mainly in a non-covalent fashion.[43] Targeting the minor groove of DNA through binding to a small molecule has long been considered an important tool in molecular recognition of a specific DNA-sequence.[44]

In our experiment, rigid molecular docking (two interacting molecules were treated as rigid bodies) studies were performed to predict the binding modes of complex **1** with a DNA duplex of sequence $d(CGCGAATTCGCG)_2$ dodecamer (PDB ID : 1BNA), and provide an energetically favorable docked pose that is shown in Fig. 7. The result shows that complex **1** interacts

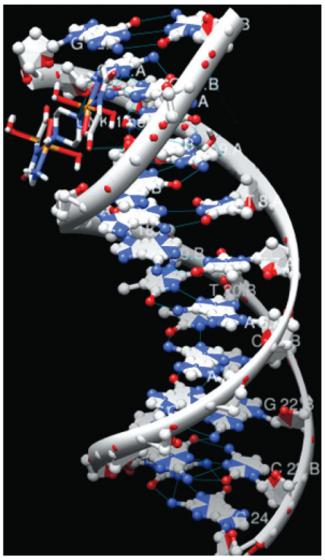

Fig. 7 A molecular docked model of complex **1** showing chemically significant hydrogen-bonding interactions into adjacent C:G base pairs from the minor side with a DNA dodecamer duplex of sequence d $(CGCGAATTCGCG)_2$ (PDB ID: 1BNA).

with DNA *via* an electrostatic mode involving outside edge stacking interactions with the oxygen atom of the phosphate backbone of DNA. In this model, it is clearly indicated that complex **1** fits snugly into the curved contour of the targeted DNA in the minor groove and is situated within a G–C rich region, thus leading to van der Waals interaction and hydrophobic contacts with DNA functional groups that define the groove.[45] Moreover, the piperazine ring of the complex **1** arranged in a parallel fashion with respect to the deoxyribose groove walls of the DNA and was stabilized by hydrogen bonding (2.8–3.0 Å) between NH of piperazine with N3 and anomeric oxygen of deoxyribose of G16B and O2 of C10A with amino functionality of dipeptide (glygly), while the remaining amino group points outside the minor groove. The resulting relative binding energy of docked metal complexes **1** DNA was found to be −256 kJ mol^{-1}. This value is consistent with the high binding constant obtained from spectroscopic titration and groove binding in presence of minor groove binder DAPI and major groove binder MG from DNA cleavage studies.

Thus, we can conclude that there is a mutual complement between spectroscopic techniques and molecular modeling, which can provide valuable information about the mode of interaction of the complex with DNA and the conformation constraints for adduct formation.

Molecular docking with topoisomerase I

In order to further rationalize the observed Topo-I inhibitory assay with complex **1**, molecular docking studies were performed to understand the binding mode of complex **1** with the human–DNA–Topo-I complex (PDB ID: 1SC7) as depicted in Fig. 8. The X-ray crystallographic structure of the human–DNA–Topo I complex was retrieved from the Protein Data Bank in which Topo I is bound to the oligonucleotide sequence 5′-AAAAAGACTTsX-GAAAATTTTT-3′, where ‘s’ is the 5′–

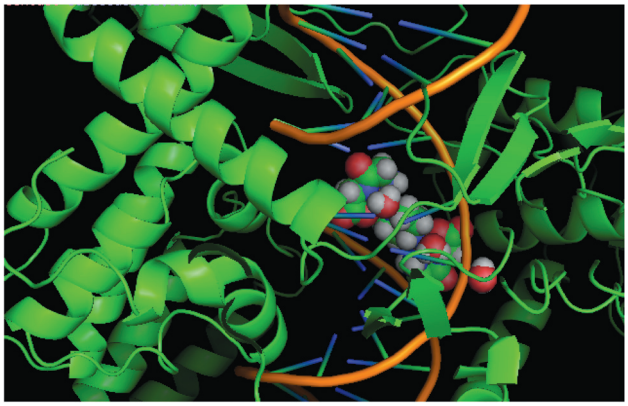

Fig. 8 A molecular docked model of complex **1** in the cleavage site of human DNA topoisomerase I (PDB ID: 1SC7).

bridging phosphorothiolate of the cleaved strand and 'X' represents any of the four bases A, G, C or T. The phosphoester bond of G12 in 1SC7 was rebuilt and the SH of G11 on the scissile strand was changed to OH.[46] The resulting docked model with minimum relative binding energy −299 kJ mol^{-1} speculates that the complex **1** intercalates between the purine ring of G11 (+1) and pyrimidine ring of T10 (−1) in the minor groove on the scissile strand and C112 and A113, on the non-scissile strand, parallel to the plane of base pairs without having hydrogen bonds with the enzyme (Fig. S5†), subsequently leading to an inhibitory effect on topoisomerase I.[47] Furthermore, DNA intercalating forces were much more important than hydrogen bonding of the ligand to the surrounding amino acids residues of the protein, or to the base pairs.[48] So, we can conclude that the complex occupies the topoisomerase binding site and may suppress the association of topoisomerase with DNA, thus influencing the topoisomerase inhibition activity or ability to form stable a complex with DNA, and have a high potential to act as a DNA-targeting anticancer drug.[49]

Molecular docking with superoxide dismutase

In order to further evaluate the SOD inhibitory assay obtained from experimental results, complex **1** was successively docked with an enzyme to search the targeted active-site (Arg141). The X-ray structure of the enzyme shows that a positively charged Arg141 is located in the outer sphere of the active site and is ~5.9 Å away from the copper ion which is coordinated by His44, His46, His61, His118, and a weakly bound water molecule which occupies the axial position of a distorted square pyramid and is directed toward the cavity opening. However, the zinc ion is completely buried in the protein, is bridged to the copper by the imidazolate side chain of His61 ion and plays a key structural role in maintaining active site structural integrity during the catalytic cycle.[50,51] Since the only access to the copper ion is from the active-site cavity, the chelators must enter the channel. This interaction would be facilitated by the positive residues lining the channel such as Arg141, Lys120, and Lys134 as illustrated in Fig. S6.† The resulting docked model clearly indicated that the dipeptide carbonyl group of complex **1** can coordinate to the active-site copper as well as the guanidyl cation of Arg141 and positively charged ammonia ion of Lys134 amino

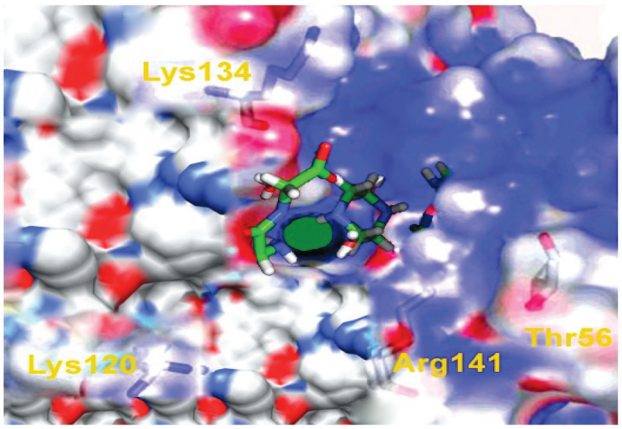

Fig. 9 Docking of complex **1** into the active-site channel demonstrates that a carbonyl group of the complex can access the active-site copper. An electrostatic loop consisting of the positively charged side chains of Arg141, Lys120, and Lys134 guides the anionic superoxide substrate to the copper center. Arg141 and Thr135 act as a "bottleneck" for the active site, limiting the access of bulky anions to the copper shown as a green sphere at the bottom of the active-site channel.

acid residues surrounding the active redox center of SOD (*i.e.*, the Cu^{2+}) (Fig. 9). In addition, the concentration of positive electrostatic potential around the channel facilitates the binding of anionic ligands in the cavity.[52]

Hence, in design for SOD mimic using binuclear copper complexes with dipeptide ligands through the hydrogen bonding moiety near the outer coordination sphere of the copper site may be essential for SOD activity.

Experimental section

Reagents and materials

All reagents were of the best commercial grade and were used without further purification. Piperazine hexahydrate (Sigma), $Cu(NO_3)_2{\cdot}3H_2O$ (Fisher Scientific), glycyl glycine (Loba chemie), Tris(hydroxymethyl)aminomethane or Tris buffer (Sigma), 6X loading dye (Fermental Life Science) and Super coiled plasmid DNA pBR322 (Genei) were utilized as received. Disodium salt of calf thymus (CT DNA) DNA purchased from Sigma Chemical Company was stored at 4 °C. Doubly distilled water was used as the solvent throughout the experiments.

Methods and instrumentation

Carbon, hydrogen and nitrogen contents were determined using Carlo Erba Analyzer Model 1108. Molar conductance was performed at room temperature on a Digisun Electronic conductivity Bridge. Fourier-transform IR (FTIR) spectra were recorded on an Interspec 2020 FTIR spectrometer. Electronic spectra were recorded on UV-1700 PharmaSpec UV-vis spectrophotometer (Shimadzu). Data were reported in λ_{max}/nm. The EPR spectrum of the copper complex was acquired on a Varian E 112 spectrometer using X-band frequency (9.1 GHz) at liquid nitrogen temperature in solid state using tetracyanoethylene (TCNE) as field marker. Interaction of the complex with calf thymus DNA

was performed in 0.01 M buffer (pH 7.2). Solutions of calf thymus DNA in buffer gave a ratio of absorbance at 260 nm and 280 nm of *ca.* 1.9 indicating that DNA was free from protein. Cleavage experiments were performed with the help of Axygen electrophoresis supported by a Genei power supply with a potential range of 50–500 V, visualized and photographed by Vilber-INFINITY gel documentation system.

Synthesis of $[Cu_2(glygly)_2(ppz)(H_2O)_4]\cdot 2H_2O$ (1)

To a stirred methanolic solution (15 ml) of $Cu(NO_3)_2\cdot 3H_2O$ (0.483 g, 0.002 mol) was added an aqueous solution of glycyl glycine (0.26 g, 0.002 mol) followed by drop wise addition of KOH (0.224 g, 0.004 mol) and the pH of the resulting solution was adjusted between 8.0 and 12. This reaction mixture was stirred for *ca.* 2 h at room temperature to obtain a clear blue color solution. A methanolic solution (10 cm^3) of piperazine hexahydrate (0.194 g, 0.001 mol) was added to the above reaction mixture and stirred for 3 h. The light blue colored solid precipitate which formed was filtered off under vacuum, washed thoroughly with ice cold methanol and dried *in vacuo* over anhydrous $CaCl_2$ (Yield: 0.255 g, 44%). Crystals suitable for X-ray analysis were collected after recrystallization from a mixture of MeOH–H_2O (95 : 5) after several days at room temperature. m. p. 205 ± 2 °C (dec.), Anal. Calcd for $C_{12}H_{34}Cu_2N_6O_{12}$ (%)C, 24.79; H, 5.89; N, 14.45, Found: C, 24.64; H, 5.67; N, 14.85, IR (KBr, cm^{-1}): 3398 $\nu(NH_2 + H_2O)$, 1602 $\nu(C{=}O)$, 1376 $\nu(C–N)$, 537 (Cu–O), 415 (Cu–N) Molar Conductance, Λ_M (1×10^{-3} M, H_2O): 20 Ω^{-1} cm^2 mol^{-1} (non-electrolyte) UV-vis absorption: λ_{max} (H_2O, 10^{-4} M), nm ($\varepsilon/10^3$ M^{-1} cm^{-1}) 232 (1.50), 278 (4.70) and 644 (2.50).

X-ray crystallography

Single crystal X-ray structural studies of the complex were performed on a Bruker SMART instrument equipped with a CCD-based detector at 298(2) K using graphite monochromated Mo Kα radiation (λ = 0.71073 Å).[53] Data collections and their refinement were evaluated by using the Bruker SMART software. The collected data were reduced by using the program SAINT,[54] and empirical absorption corrections were done using the SADABS.[55] The structure was solved by direct methods and refined with the full-matrix least squares techniques using SHELX-97.[56] The positions of all atoms were obtained by direct methods. Anisotropic thermal parameters were assigned to all non-hydrogen atoms and the remaining hydrogen atoms were placed in geometrically constrained positions and refined as riding atoms with a common fixed isotropic thermal parameter. ORTEP3 was used to produce graphical representation.[57] A summary of the selected crystallographic information is given in Table 1.

DNA-binding and cleavage experiments

DNA binding experiments include absorption spectral traces, emission spectroscopy and circular dichroism conformed to the standard methods and practices previously adopted by our laboratory.[58–61] While measuring the absorption spectra an equal amount of DNA was added to the compound solution and the reference solution to eliminate the absorbance of the CT DNA itself, and the CD contribution by the CT DNA and Tris buffer was subtracted through base line correction.

The cleavage experiments of supercoiled pBR322 DNA (300 ng) by complex **1** (10–30 μM) in Tris-HCl–NaCl (5 : 50 mM) buffer at pH 7.2 were carried out using agarose gel electrophoresis. The samples were incubated for 45 min at 310 K. A loading buffer containing 25% bromophenol blue, 0.25% xylene cyanol, 30% glycerol was added and electrophoresis was carried out at 50 V for 1 h in Tris-HCl buffer using 1% agarose gel containing 1.0 mg ml^{-1} ethidium bromide. The DNA cleavage with added reductant was monitored as in the case of the cleavage experiment without added reductant using agarose gel electrophoresis.

Table 1 Selected crystallographic data for the complex **1**

Parameter	
Formula	$C_{12}H_{34}Cu_2N_6O_{12}$
Fw (g mol^{-1})	581.55
Cryst syst	Monoclinic
Space group	$P21/c$
a (Å)	8.704 (4)
b (Å)	10.611 (5)
c (Å)	12.345 (5)
α (°)	90
β (°)	105.085
γ (°)	90
V ($Å^3$)	1100 (9)
Z	2
D_{calc} (Mg m^{-3})	1.754
μ (mm^{-1})	2.003
F (000)	604.0
Crystal size (mm)	0.15 × 0.14 × 0.12
Temp (K)	298(2)
Measured reflns	9480
Unique reflns	1943
θ Range (°)/completeness (%)	2.42 to 25.00
No. of data/parameters/restraints	1943/172/0
GoF[a]	0.981
$R^b[I > 2\sigma(I)]$	0.0418
$wR_2{}^b$ (all data)	0.1006
Largest diff. peak/hole (e $Å^{-3}$)	0.478/−0.405

[a] GoF is defined as $\{\Sigma[w(F_o^2 - F_c^2)]/(n-p)\}^{1/2}$ where n is the number of data and p is the number of parameters. [b] $R = \{\Sigma||F_o| - |F_c|| / \Sigma|F_o|$, $wR_2 = \{\Sigma w(F_o^2 - F_c^2)^2/\Sigma w(F_o^2)^2\}^{1/2}$.

Topoisomerase I inhibition assay

DNA topoisomerase I, Human (Topo-I) was purchased from CALBIOCHEM and was used without further purification. One unit of the enzyme was defined as completely relaxed 1 μg of negatively supercoiled pBR322 DNA in 30 min at 310 K under the standard assay conditions. The reaction mixture (30 μL) contained 35 mM Tris-HCl (pH 8.0), 72 mM KCl, 5 mM $MgCl_2$, 5 mM DTT, 2 mM spermidine, 0.1 mg mL^{-1} BSA, 0.25 μg pBR322 DNA, 2 Unit Topo I and complex **1**. These reaction mixtures were incubated at 310 K for 30 min, and the reaction was terminated by addition of 4 μL of 5× buffer solution consisting of 0.25% bromophenol blue, 4.5% SDS and 45% glycerol. The samples were electrophoresed through 1% agarose in TBE at 30 V for 8 h.

Molecular docking

The rigid molecular docking studies were performed using HEX 6.1 software,[62] an interactive molecular graphics program for calculating and displaying feasible docking modes of pairs of protein, enzymes and DNA molecule. The coordinates of the metal complex were taken from its crystal structure as a CIF file and were converted to the PDB format using Mercury software. The crystal structure of the B–DNA dodecamer d $(CGCGAATTCGCG)_2$ (PDB ID: 1BNA), native SOD (PDB ID: 1SXA) and human–DNA–Topo I complex (PDB ID: 1SC7) were downloaded from the protein data bank. All calculations were carried out on an Intel pentium4, 2.4 GHz based machine running MS Windows XP SP2 as the operating system. Visualization of the docked pose have been done using CHIMERA[63] and PyMol[64] molecular graphics programs.

Determination of the superoxide dismutase activity

Superoxide dismutase activity of the complex **1** was assayed by using its ability to inhibit the reduction of nitroblue tetrazolium, NBT, at 560 nm by superoxide ions produced by the xanthine–xanthine oxidase system.[65–67] The assay was carried out in the assay buffer containing 50 mM Tris-HCl, pH 8.0, 0.1 mM diethylene triamine penta acetic acid (DTPA) and 0.1 mM hypoxanthine. The radical detector consists of a tetrazolium salt and is diluted by assay buffer. Similarly, the solutions of SOD standards and xanthine oxidase were prepared in sample buffer consisting of 50 mM Tris-HCl, pH 8.0. The SOD mimetic activity of the tested copper complex in aqueous solution at 25 °C was evaluated from the absorbance decrease at 560 nm comparing to the blank (the reaction mixture without the copper complex). The concentration of complex required to yield 50% inhibition of NBT reduction (the IC_{50} value) was determined from a plot of percentage inhibition *versus* copper complex concentration (μM).

Conclusions

In this work, we have designed and synthesized a new dinuclear copper(II) complex derived from the dipeptide (glygly) and piperazine as a metallopeptide drug to examine their effect on the binding propensity of DNA and to elucidate the mechanism of action at the molecular target. The *in vitro* DNA binding studies of complex **1** reveal an electrostatic mode of binding as well as selective binding to the minor groove of DNA. The complex **1** cleaves supercoiled plasmid DNA through an oxidative (O_2-pathway) cleavage mechanism induced by a reactive oxygen species (ROS). Furthermore, complex **1** exhibits significant inhibitory effects on Topo-I activity at a very low concentration, ~12.5 μM, including excellent SOD mimics with an IC_{50} of 0.086 μM. Additionally, molecular docking studies were performed with molecular target DNA and the active site of enzymes in order to validate the experimental results. Therefore, it is concluded that drugs that bind to the DNA minor groove and inhibit DNA-processing enzymes represent an important class of anticancer drugs.

Acknowledgements

We express our gratitude to DBT, New Delhi, for generous financial support (Scheme no. BT/PR6345/MED/14/784/2005). Thanks to RSIC, CDRI Lucknow for providing CHN analysis data and for Single Crystal Diffractometer facility at Missouri University of Science and Technology, USA.

Notes and references

1 H. Brody, Cancer prevention, *Nature Outlook*, 2011, **471**, S1.
2 L. Dalla Via, S. Marciani Magno, O. Gia, A. M. Marini, F. D. Settimo, S. Salerno, C. La Motta, F. Simorini, S. Taliani, A. Lavecchia, C. Di Giovanni, G. Brancato, V. Barone and E. Novellino, *J. Med. Chem.*, 2009, **52**, 5429.
3 (*a*) B. Rosenberg, *Interdisciplinary Science Reviews*, 1978, **3**, 134; (*b*) B. Rosenberg, L. VanCamp, J. E. Trosko and V. H. Mansour, *Nature*, 1969, **222**, 385.
4 G. Facchin, E. Kremer, D. A. Barrio, S. B. Etcheverry, A. J. Costa-Filho and M. H. Torre, *Polyhedron*, 2009, **28**, 2329.
5 M. Singh and V. Tandon, *Eur. J. Med. Chem.*, 2011, **46**, 659.
6 (*a*) Y. Pommier, P. Pourquier, Y. Fan and D. Strumberg, *Biochim. Biophys. Acta, Gene Struct. Expression*, 1998, **1400**, 83; (*b*) J. J. Champoux, *Annu. Rev. Biochem.*, 2001, **70**, 369.
7 C. Bailly, *Curr. Med. Chem.*, 2000, **7**, 39.
8 C. Bailly and J. B. Chaires, *Bioconjugate Chem.*, 1998, **9**, 513.
9 (*a*) M. L. Lopez-Rodrıguez, M. J. Morcillo, E. Fernandez, B. Benhamu, I. Tejada, D. Ayala, A. Viso, M. Olivella, L. Pardo, M. Delgado, J. Manzanaresd and J. A. Fuentesd, *Bioorg. Med. Chem. Lett.*, 2003, **13**, 1429; (*b*) J. M. Domagala, A. J. Bridges, T. P. Culbertson, L. Gambino, S. E. Hagen, G. Karrick, K. Porter, J. P. Sanchez, J. A. Sesnie, F. G. Spense, D. Szotek and J. Wemple, *J. Med. Chem.*, 1991, **34**, 1142.
10 (*a*) M. L. Lopez-Rodriguez, M. J. Morcillo, E. Fernandez, M. L. Rosado, L. Orensanz, M. E. Beneytez, J. Manzanares, J. A. Fuentes and K. J. Schaper, *Bioorg. Med. Chem. Lett.*, 1999, **9**, 1679; (*b*) M. Hagibara, H. Kashiwase, T. Katsube, T. Kimura, T. Komai, K. Momota, T. Ohmine, T. Nishigaki, S. Kimura and K. Shimada, *Bioorg. Med. Chem. Lett.*, 1999, **9**, 3063.
11 C. A. Claussen and E. C. Long, *Chem. Rev.*, 1999, **99**, 2797.
12 T. Kieber-Emmons, R. Murli and M. I. Green, *Curr. Opin. Biotechnol.*, 1997, **8**, 435.
13 Y. Fujii, T. Kiss, T. Gajda, X. S. T. T. Sato, Y. N. Y. Hayashi and M. Yashiro, *JBIC, J. Biol. Inorg. Chem.*, 2002, **7**, 843.
14 A. R. Paital, D. Mandal, X. Huang, J. Li, G. Aromí and D. Ray, *Dalton Trans.*, 2009, 1352.
15 M. Bera, J. Ribas, W. T. Wong and D. Ray, *Inorg. Chem. Commun.*, 2004, **7**, 1242.
16 M. D. P. Brandi-Blanco, D. Choquesillo-Lazarte, A. Domínguez-Martín, J. M. González-Pérez, A. Castiñeiras and J. Niclós-Gutiérrez, *J. Inorg. Biochem.*, 2011, **105**, 616.
17 J. Dehand, J. Jordanov, F. Keck, A. Mosset, J. J. Bonnet and J. Galy, *Inorg. Chem.*, 1979, **18**, 1543.
18 M. Tiliakos, E. Katsoulakou, V. Nastopoulos, A. Terzis, C. Raptopoulou, P. Cordopatis and E. Manessi-Zoupa, *J. Inorg. Biochem.*, 2003, **93**, 109.
19 E. Manessi-Zoupa, S. P. Perlepes, V. Hondrellis and J. M. Tsangaris, *J. Inorg. Biochem.*, 1994, **55**, 217.
20 H. Sigel and R. B. Martin, *Chem. Rev.*, 1982, **82**, 385.
21 I. A. Koval, M. Sgobba, M. Huisman, M. Luken, E. Saint-Aman, P. Gamez, B. Krebs and J. Reedijk, *Inorg. Chim. Acta*, 2006, **359**, 4071.
22 (*a*) B. J. Hathaway and D. E. Billing, *Coord. Chem. Rev.*, 1970, **5**, 143; (*b*) A. M. Herrera, R. J. Staples, S. V. Kryatov, A. Y. Nazarenko and E. V. Akimova, *Dalton Trans.*, 2003, 846.
23 D. Kivelson and R. R. Neiman, *J. Chem. Phys.*, 1961, **35**, 149.
24 S. Chandra and X. Sangeetika, *Spectrochim. Acta, Part A*, 2004, **60**, 147.
25 H. L. Chan, Q. L. Liu, B. C. Tzeng, Y. S. You, S. M. Peng, M. Yang and C. M. Che, *Inorg. Chem.*, 2002, **4**, 13161.
26 E. C. Long and J. K. Barton, *Acc. Chem. Res.*, 1990, **23**, 271.
27 J. K. Barton, A. T. Danishefsky and J. M. Goldberg, *J. Am. Chem. Soc.*, 1984, **106**, 2172.
28 J. Olmsted and D. R. Kearns, *Biochemistry*, 1977, **16**, 3647.
29 B. C. Baguley and M. L. Bret, *Biochemistry*, 1984, **23**, 937.

30 R. Indumathy, S. Radhika, M. Kanthimathi, T. Weyhermuller and B. U. Nair, *J. Inorg. Biochem.*, 2007, **101**, 434.
31 V. I. Ivanov, L. E. Minchenkova, A. K. Schyolkina and A. I. Poletayer, *Biopolymers*, 1973, **12**, 89.
32 N. Grover, N. Gupta, P. Singh and H. H. Thorp, *Inorg. Chem.*, 1992, **31**, 2014.
33 S. Mahadevan and M. Palaniandavar, *Inorg. Chem.*, 1998, **37**, 693.
34 J. K. Barton, A. T. Danishefsky and J. M. Goldberg, *J. Am. Chem. Soc.*, 1984, **106**, 2172.
35 D.-D. Li, J.-L. Tian, W. Gu, X. Liu, H.-H. Zeng and S.-P. Yan, *J. Inorg. Biochem.*, 2011, **105**, 894.
36 F. Arjmand, M. Muddassir and R. H. Khan, *Eur. J. Med. Chem.*, 2010, **45**, 3549.
37 F. V. Pamatong, C. A. Detmer III and J. R. Bocarsly, *J. Am. Chem. Soc.*, 1996, **118**, 5339.
38 B. Montaner, W. Castillo-Avila, M. Martinell, R. Ollinger, J. Aymami, E. Giralt and R. Perez-Tomas, *Toxicol. Sci.*, 2005, **85**, 870.
39 L. F. Chin, S. M. Kong, H. L. Seng, K. S. Khoo, R. Vikneswaran, S. G. Teoh, M. Ahmad, S. B. A. Khoo, M. J. Maah and C. H. Ng, *J. Inorg. Biochem.*, 2011, **105**, 221.
40 I. Fridovich, *Annu. Rev. Biochem.*, 1975, **44**, 147.
41 G. Facchin, M. H. Torre, E. Kremer, O. E. Piro, E. E. Castellano and E. J. Baran, *J. Inorg. Biochem.*, 2002, **89**, 174.
42 A. L. Abuhijleh, *J. Inorg. Biochem.*, 1997, **68**, 167.
43 R. Rohs, I. Bloch, H. Sklenar and Z. Shakked, *Nucleic Acids Res.*, 2005, **33**, 7048.
44 L. F. Pineda De Castro and M. Zacharias, *J. Mol. Recognit.*, 2002, **15**, 209.
45 R. Filosa, A. Peduto, S. Di Micco, P. de Caprariis, M. Festa, A. Petrella, G. Capranico and G. Bifulco, *Bioorg. Med. Chem.*, 2009, **17**, 13.
46 B. L. Staker, M. D. Feese, M. Cushman, Y. Pommier, D. Zembower, L. Stewart and A. B. Burgin, *J. Med. Chem.*, 2005, **48**, 2336.
47 H. T. M. Van and W.-J. Cho, *Bioorg. Med. Chem. Lett.*, 2009, **19**, 2551.
48 X. S. Xiao and M. Cushman, *J. Am. Chem. Soc.*, 2005, **127**, 9960.
49 Y. Pommier, *Nat. Rev. Cancer*, 2006, **6**, 789.
50 W. R. Rypniewski, S. Mangani, B. Bruni, P. L. Orioli, M. Casati and K. S. Wilson, *J. Mol. Biol.*, 1995, **251**, 282.
51 J. A. Tainer, E. D. Getzoff, J. S. Richardson and D. C. Richardson, *Nature*, 1983, **306**, 284.
52 M. Ye and A. M. English, *Biochemistry*, 2006, **45**, 12723.
53 C. Piguet, G. Bernardinelli and G. Hopfgartner, *Chem. Rev.*, 1997, **97**, 2005.
54 Siemens, SMART and SAINT, *Area Detector Control and Integration Software*, Siemens Analytical X-Ray Systems, Inc., Madison, Wisconsin, USA, 1996.
55 Siemens, SHELXTL, Version 5 Reference Manual, Siemens Analytical X-ray Systems, Inc., Madison, Wisconsin, USA, 1996.
56 G. M. Sheldrick, *Acta Crystallogr., Sect. A: Found. Crystallogr.*, 2008, **A64**, 112–122; *Program for Crystal Structure Solution and Refinement*, University of Goettingen, Germany, 1997.
57 L. J. Farrugia, *J. Appl. Crystallogr.*, 1997, **30**, 565.
58 J. Marmur, *J. Mol. Biol.*, 1961, **3**, 208.
59 M. E. Reicmann, S. A. Rice, C. A. Thomas and P. Doty, *J. Am. Chem. Soc.*, 1954, **76**, 3047.
60 A. Wolfe, G. H. Shimer and T. Meehan, *Biochemistry*, 1987, **26**, 6392.
61 J. R. Lakowiez and G. Webber, *Biochemistry*, 1973, **12**, 4161.
62 D. Mustard and D. W. Ritchie, *Proteins: Struct., Funct., Bioinf.*, 2005, **60**, 269.
63 E. F. Pettersen, T. D. Goddard, C. C. Huang, G. S. Couch, D. M. Greenblatt, E. C. Meng and T. E. Ferrin, *J. Comput. Chem.*, 2004, **25**, 1605.
64 W. L. DeLano, *The PyMOL Molecular Graphics System*, DeLano Scientific, San Carlos, CA, USA, 2002.
65 D. K. Demertzi, A. Galani, M. A. Demertzis, S. Skoulika and C. Kotoglou, *J. Inorg. Biochem.*, 2004, **98**, 358.
66 A. L. Abuhijleh and C. Woods, *Inorg. Chem. Commun.*, 2002, **5**, 269.
67 G. Lupidi, F. Marchetti, N. Masciocchi, D. L. Reger, S. Tabassum, P. Astolfi, E. Damiani and C. Pettinari, *J. Inorg. Biochem.*, 2010, **104**, 820.

